ChemPubSoc Europe

DOI: 10.1002/cbic.201700457

CHEMBIOCHEM Full Papers

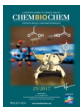

Towards Tuneable Retaining Glycosidase-Inhibiting Peptides by Mimicry of a Plant Flavonol Warhead

Ryoji Yoshisada, Lieke van Gijzel, and Seino A. K. Jongkees*[a]

Retaining glycosidases are an important class of enzymes involved in glycan degradation. To study better the role of specific enzymes in deglycosylation processes, and thereby the importance of particular glycosylation patterns, a set of potent inhibitors, each specific to a particular glycosidase, would be an invaluable toolkit. Towards this goal, we detail here a more in-depth study of a prototypical macrocyclic peptide inhibitor of the model retaining glycosidase human pancreatic α-amylase (HPA). Notably, incorporation of L-DOPA into this peptide affords an inhibitor of HPA with potency that is tenfold higher (K_i = 480 pM) than that of the previously found consensus sequence. This represents a first successful step in converting a recently discovered natural-product-derived motif, already specific for the catalytic side-chain arrangement conserved in the active sites of retaining glycosidases, into a tuneable retaining glycosidase inhibition warhead.

Introduction

Carbohydrates are important for many cellular recognition and communication processes, and thus aberrant carbohydrate processing can lead to many disease states.[1] The addition and removal of carbohydrates from biomolecules in a cellular setting is performed by carbohydrate-active enzymes, a term encompassing both the enzymes that add monomers to a glycan, such as glycosyl transferases, and the enzymes that remove them, such as glycoside hydrolases (glycosidases).[2] Regulation of the production, maturation, and activity of these enzymes in turn regulates the flux of glycan processing and, thus, determines the presentation of different glycans on cells.[3] The interplay between these different enzymatic activities is complex, and it can be difficult to determine the role of a single enzyme or a single glycan.

One approach that would allow dissection of these glycan-processing pathways is through the use of selective and high-affinity inhibitors of the various enzymes involved.[4] However, because many glycosidases share structural and mechanistic features, "traditional" transition-state mimic inhibitors can be difficult to make selective for a single enzyme.[5] As an alternative approach, we are attempting to develop de novo macrocyclic peptide inhibitors that are specific to a given carbohydrate-active enzyme through the use of a technology called the RaPID (random nonstandard peptide integrated discovery) system,[6] a form of mRNA display incorporating genetic-code reprogramming. Because of the large number of specific contacts with their targets, peptides derived by using this system have often been found to bind with low-nanomolar potency and high selectivity,[7–9] including for isoforms.[10] A set of peptide inhibitors against different glycan-processing enzymes derived by using this system would prove a valuable toolkit to allow the unravelling of this complex web of modification pathways.

To target binding of such peptides to the active site of retaining glycosidases and glycosyl transferases, we are attempting to incorporate the recently characterised two-part warhead of the natural-product inhibitor montbretin A (Figure 1)[11] into the RaPID system. Montbretin A presents the catechol- and resorcinol-containing moieties caffeic acid and myricetin in an offset stacked conformation that strongly binds to the catalytic residues of the retaining glycosidase human pancreatic α-amylase (HPA; EC 3.2.1.1). Because the three-dimensional arrangement of catalytic residues is largely conserved across the retaining glycosidases,[12] it is our hope that if mimics of caffeic acid and myricetin could be appropriately presented in a peptide context it would allow tuning of inhibitor affinity to target different enzymes selectively. Inhibitors of HPA are also of relevance to treatment of type 2 diabetes[13] as a means of preventing starch breakdown into glucose and, thus, limiting total glucose intake to prevent blood-sugar spikes.

To test whether the peptide scaffold could appropriately arrange these functional groups in three-dimensional space, we previously performed a RaPID selection against HPA,[14] the enzyme with which montbretin A was discovered,[15] but also a model retaining glycosidase that is of clinical relevance for the prevention of type 1 diabetes mellitus.[16] HPA has been rigorously studied in the past, including by X-ray crystallography,[17,18] mechanistic dissection,[19] and the discovery of inhibitors based on transition-state mimicry,[20] proteins,[21–24] and natural products,[11] which together provide many points of comparison. The key functional elements of the two-part warhead of montbretin A were incorporated into a peptide library

[a] R. Yoshisada, L. van Gijzel, Dr. S. A. K. Jongkees
Department of Chemical Biology and Drug Discovery
Utrecht Institute of Pharmaceutical Sciences, Utrecht University
Universiteitsweg 99, Utrecht 3584CG (The Netherlands)
E-mail: s.a.k.jongkees@uu.nl

Supporting Information and the ORCID identification numbers for the authors of this article can be found under https://doi.org/10.1002/cbic.201700457.

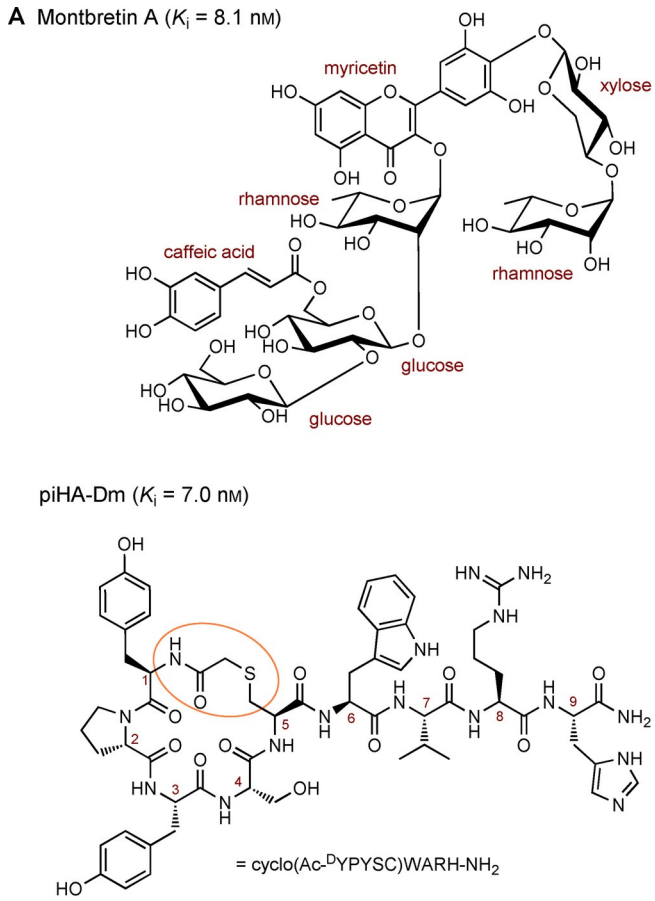

Figure 1. A) Chemical structures of montbretin A and piHA-Dm, B) secondary structure of piHA-Dm and C) its binding in the HPA active site (PDB ID: 5KEZ).[14] Residues are labelled in red, and the peptide thioether macrocyclisation is circled in yellow. Peptide residues are shown in orange, and HPA residues are shown in wheat tint, with heteroatoms coloured red for oxygen, blue for nitrogen, and yellow for cysteine.

design, the catechol as an L-DOPA residue by genetic-code reprogramming to replace methionine ("d" in sequence alignments) and a simple resorcinol as a post-translational modification on free cysteines,[25] with the hope that selective pressure for binding to the target would drive these to an appropriate arrangement to mimic their placement in montbretin A. Unfortunately, neither of the desired moieties were present in the most-abundant selected peptide sequences, despite rapid enrichment of a tight binding peptide inhibitor. In this work, we aim to understand better this "peptide inhibitor of human α-amylase" (piHA, Figure 1) and its interactions with HPA, and we focus on the possibility for incorporation of a montbretin-like warhead into a peptide inhibitor scaffold.

Results and Discussion

Peptide truncations and solution conformation

In the previously reported selection work, the library used was composed of an immutable initiating residue of *N*-chloroacetyl-D- or -L-tyrosine (two parallel selections) that was followed by 15 freely varying amino-acid positions and finally a conserved cysteine, which afforded spontaneous head-to-side-chain macrocyclisation with the chloroacetyl group.[26] Sequencing of the enriched library revealed that a unique lariat nonapeptide consensus sequence of ^{D}YPYSCWVRH was present only in the D-tyrosine initiated library, and truncation to only this consensus (named with the suffix "Dm") gave inhibition comparable to that of the parent sequence (Table 1). Here, we report that further truncation of piHA-Dm to only the macrocycle furnished a compound that showed no inhibition activity, illustrating the important role of the short tail of this lariat structure for tight binding. Furthermore, truncation of the slightly higher affinity piHA-D1 sequence to the nonapeptide consensus (removing residues 10–15), effectively a V7A substitution in piHA-Dm, resulted in an approximately threefold improvement in affinity. Truncating one fewer amino acids (removing residues 11–15, equivalent to adding Val10 to this V7A variant) gave little additional benefit. These truncations showed that the full consensus sequence was necessary and sufficient for tight binding of this peptide to HPA.

Table 1. Inhibition data for piHA truncations.

Abbreviation	Structure/sequence	K_i [nM]
piHA-D1	cyclo(Ac-^{D}YPYSC)WARHVRIREN-NH_2	1.0 ± 0.1[14]
piHA-D3	cyclo(Ac-^{D}YPYSC)WVRHSDPHKF-NH_2	2.7 ± 0.7[14]
piHA-Dm	cyclo(Ac-^{D}YPYSC)WVRH-NH_2	7.0 ± 3.5[14]
piHA-D1-Δ10-15	cyclo(Ac-^{D}YPYSC)WARH-NH_2	2.0 ± 0.3
piHA-D1-Δ11-15	cyclo(Ac-^{D}YPYSC)WARHV-NH_2	1.3 ± 0.2
piHA-Dm-Δ6-9	cyclo(Ac-^{D}YPYSC)-NH_2	$\gg 5000$[a]
piHA-Dm-(lin)	Ac-^{D}YPYSAWVRH-NH_2	70 ± 30[b]

[a] No inhibition detected up to 5 μM. [b] IC_{50} value.

In contrast to the dramatic effect of further truncation, a linear analogue of the full-length piHA-Dm sequence did retain a substantial proportion of its activity, which decreased approximately tenfold. Such a drop in activity is not uncommon for macrocyclic peptide ligands from in vitro selection upon conversion into their linear analogues.[7,9] This is typically attributed to preorganisation of the ligand in the binding conformation, which reduces the entropic cost of binding, but very few solution structures of macrocyclic peptides from in vitro selection have been reported to support this.[27] To investigate whether the 3_{10}-helical conformation seen in our previously reported crystal structure of piHA-Dm[14] was also present if the peptide was free in solution, we probed its folding behaviour by using circular dichroism (CD; Figure 2).

Literature reports for the CD spectra of 3_{10}-helices feature a strong negative band at approximately $\lambda = 205$ nm,[28–30] but

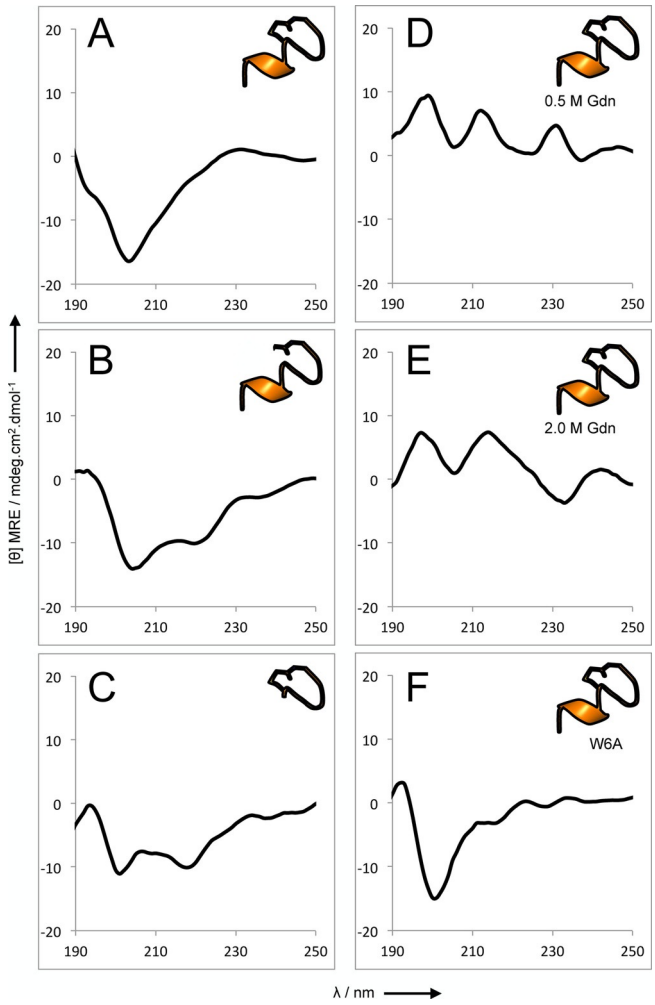

Figure 2. CD spectra of A) piHA-Dm, B) piHA-Dm-(lin), C) piHA-Dm-Δ6-9, D) piHA-Dm with 0.5 M guanidinium hydrochloride, E) piHA-Dm with 2.0 M guanidinium hydrochloride, and F) piHA-Dm-W6A.

outside of this, spectral patterns are variable, as these helices are generally transient structural features on a folding pathway towards an α helix (itself characterised by negative bands at $\lambda = 208$ and 222 nm). The CD spectrum of the full-length macrocyclic piHA-Dm shows a strong negative band at $\lambda = 203$ nm, which appears distinct from a random coil in that its ellipticity rises to 0 at $\lambda = 190$ nm and the negative ellipticity continues out to $\lambda = 230$ nm. Interestingly, the CD spectrum of the linear analogue piHA-Dm-lin shows bands that are more characteristic of an α helix, unusual for such a short linear peptide, as does the truncated macrocycle-only peptide piHA-Dm-Δ6-9. This indicates that these peptides fold into well-defined secondary structure elements if free in solution for both the macrocyclic and the linear portions of the peptide. The solution structure of the full-length lariat peptide is thus distinct from both the macrocycle-only and the linear analogues and is consistent with the formation of a 3_{10}-helix. This feature is presumed to be favoured by both the short length of the helix and a template effect by the macrocycle. Furthermore, the addition of the chaotropic agent guanidinium hydrochloride to 0.5 M resulted in a dramatic shift in the CD spectrum of piHA-Dm, but additional chaotropic salt did not give any substantial further change, thus suggesting that this fold is relatively easily disrupted. These results stand in contrast to those reported for a set of disuccinimidyl glutarate macrocyclised peptides targeting the signalling protein Gαi1-GDP, for which there was no evidence of any folding in solution for either the linear or macrocyclic forms, and they gave almost identical spectra.[31]

Alanine scanning

To investigate further the contribution of each amino acid to binding, an alanine scan of the piHA-Dm peptide was performed (Table 2). In this, marked differences in inhibition were observed for all mutations, which again stands in contrast to a similar selected macrocyclic peptide inhibitor,[7] wherein most single alanine substitutions had only minor effects. This indicates an unusually high residue efficiency for piHA-Dm in its interactions with HPA and can largely be rationalised in terms of the dense network of intermolecular hydrogen bonds between HPA and piHA-Dm described previously.[14] The following should be noted: 1) the invariant initiating amino acid Tyr1 makes a substantial contribution to binding despite not being allowed to optimise during the selection, 2) the side chain of Pro2 appears to make a hydrophobic interaction that also contributes to binding, 3) the interaction of Tyr3 with the HPA catalytic nucleophile Asp197 is critical for strong binding, 4) the hydrogen bond of Ser4 is a less-important contributor to binding, 5) the solvent-exposed Arg8/His9 pair interacts strongly with HPA Asp356. These values also correlate well with the observation that removal of the linear tail of the peptide gives a molecule with very poor inhibition, as three of the four amino acids in this tail give binding that is over two orders of magnitude poorer if mutated to alanine.

Table 2. Inhibition data for piHA-Dm alanine scan.

Abbreviation	Structure/sequence	IC_{50} [nM]
piHA-Dm-y1a	cyclo(Ac-^{D}APYSC)WVRH-NH_2	1200 ± 300
piHA-Dm-P2A	cyclo(Ac-^{D}YAYSC)WVRH-NH_2	470 ± 100
piHA-Dm-Y3A	cyclo(Ac-^{D}YPASC)WVRH-NH_2	≫ 5000[a]
piHA-Dm-S4A	cyclo(Ac-^{D}YPYAC)WVRH-NH_2	200 ± 30
piHA-Dm-W6A	cyclo(Ac-^{D}YPYSC)AVRH-NH_2	3200 ± 400
piHA-Dm-R8A	cyclo(Ac-^{D}YPYSC)WVAH-NH_2	1100 ± 200
piHA-Dm-H9A	cyclo(Ac-^{D}YPYSC)WVRA-NH_2	1500 ± 300

[a] No inhibition detected up to 5 μM.

The large drop in affinity observed for the W6A mutant is more difficult to rationalise. In the crystal structure of piHA-Dm bound to HPA, Trp6 is observed to make a single hydrogen bond to Thr163 and might also be involved in edge-to-face aromatic interactions with Tyr3 of piHA-Dm and Trp59 of HPA (closest interatom distances of 3.7 and 4.0 Å). No HPA amino-acid side chains are suitably placed to take part in π–π stacking or cation–π interactions (Figure 3). Alternative explanations for the large drop in affinity with the W6A mutation could be

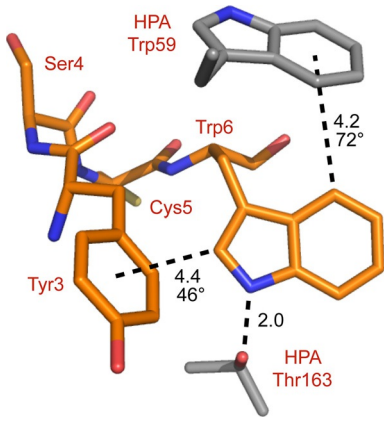

Figure 3. Interactions of piHA-Dm Trp6 (PDB ID: 5KEZ).[14] Residues are labelled in red text, and distances [Å] and angles (between planes) are shown in black. For aromatic interactions, distances are from the closest atom to the centre of the ring, as indicated. Peptide residues are shown in orange and HPA amino acids are shown in grey, with heteroatoms coloured red for oxygen, blue for nitrogen, and yellow for cysteine.

a nonspecific hydrophobic interaction or a structural role for this amino acid in the folding of the peptide. The former explanation would suggest that other hydrophobic residues such as Val, Leu, and Ile should also be tolerated, which appears not to be the case. Aromatic substitutions, on the other hand, do appear to be tolerated (see below). Measuring a CD spectrum of the piHA-Dm-W6A mutant to test the latter hypothesis revealed some deviation from that of the consensus sequence, and the spectrum is again distinct from that of piHA-Dm as well as those of its linear and macrocycle-only analogues (see above). This is indicative of a change in peptide folding in solution, and thus, folding effects provide an additional possible explanation for the importance of this residue; Trp6 may provide unexpected structural stabilisation of the peptide itself.

Deep sequencing re-analysis and L-DOPA incorporation

In the initial analysis of our selection deep sequencing,[14] we sought the most-abundant sequences and constructed a sequence logo representing amino-acid abundance at each residue position on the basis of a global analysis. Although this analysis revealed the piHA-Dm consensus, the tolerance for low-abundance substitutions at each position might also provide information on which interactions are important. The deep sequencing dataset from the third round of our previously reported selection, for which library enrichment was first apparent, was searched for sequences with single-residue mismatches to the consensus. In using this early round it was hoped that we could minimise the contribution of selection pressures other than target binding to sequence abundance. In that sequencing dataset, from a total of 135 385 valid sequences (no internal stop codons, correct transcription start, ribosome binding, and mRNA display linker binding sites), there were 25 533 exact matches to the consensus ^{D}YPYSCWXRH, whereas allowing a single further mismatch outside of nonconserved position 7 increased this to 45 794 sequences (34% of total sequences).

A full analysis of per-residue variation is presented in Figure 4, which shows all single substitutions at each position in the consensus sequence. From this figure it is apparent that whereas all positions were well conserved, there were some

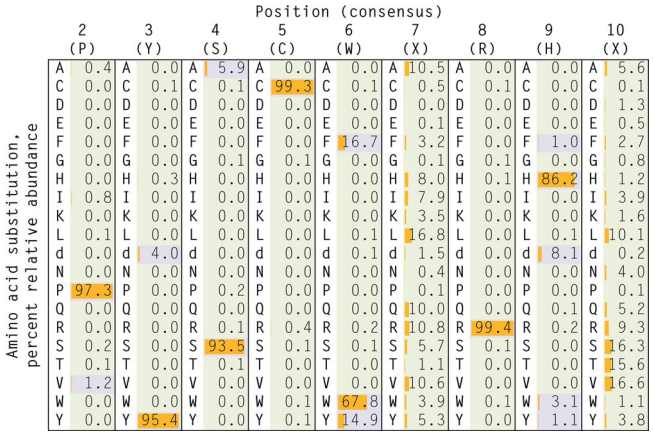

Figure 4. Abundance of each single-point mutation in the piHA-Dm consensus (peptides were prepared ribosomally as a mixed pool from a selection-enriched DNA library and were binding-affinity profiled by pull down on immobilised HPA[14]). Entries are colour coded by a yellow bar with the length proportional to the percent abundance and a lilac background for greater than 1% abundance in a conserved location ("d" = L-DOPA).

positions at which small amounts of variation appeared to be better tolerated. As most mutations appeared to be present at only a small fraction of a percentage, a cut-off of 1% of the total sequences was empirically chosen to represent some enrichment above background. This revealed the conservative mutations Pro2 to Val (1.2%); Tyr3 to DOPA (4.0%); Ser4 to Ala (5.9%); Trp6 to Phe (16.7%) or Tyr (14.9%); and His9 to Phe (1.0%), DOPA (8.1%), Trp (3.1%) or Tyr (1.1%). Positions 7 and 10 showed some amino acids having higher abundance than others but with no clear pattern of preference, as both positions exhibited aliphatic, aromatic, polar, and charged amino acids above the chosen cut-off. Only Cys5, the amino acid involved in macrocyclisation, and Arg8, which interacts with HPA Asp356, showed no tolerated substitutions above this cut-off, and this suggests that they cannot be substituted in their respective roles by any other natural amino acid.

One of the tolerated mutations, S4A, was included in the alanine scan above and so provides a possible benchmark for interpreting these trends. The S4A mutant, which was present in 5.9% of sequences, had an IC_{50} of 470 nM and is, thus, approximately 30 times less active than the consensus sequence. This mutant is around the middle of the range of sequence abundance levels observed above the chosen cut-off (1.0–16.7%). That the R8A mutant, with affinity of 1100 nM, is not tolerated implies this cut-off corresponds to an affinity between 0.5 and 1 μM and so suggests that these mutations are unlikely to be more potent than the consensus. Nonetheless, the types of mutations tolerated are informative about the interactions that are important at each position. The P2V mutant fits the above hypothesis that proline makes a beneficial hydrophobic contact with HPA, and larger hydrophobic amino

acids are likely not tolerated because of steric factors. Both Trp6 and His9 appear to tolerate substitution with almost any aromatic amino acid; this suggests that their hydrogen-bonding interactions are less important than their aromatic interactions. Whereas there is a possible edge-to-surface interaction of His6 with HPA Trp357 (4.1 Å closest atom contact), there are again no π–π stacking or cation–π interactions to be found for this residue in the crystal structure of piHA-Dm bound to HPA. Thus, our results suggest that for both Trp6 and His9 it is the aromatic interactions that are most important for binding.

Recent literature indicated that low-abundance sequences in a selection-enriched library could have greater in vitro affinity and/or biological activity than either the most-abundant sequence or the global average.[32] In the current work, because we were analysing single amino-acid variations in the same sequence, we expected that sequence conservation of the natural amino-acid mutations would correlate with affinity (as seen for S4A). However, this might not be the case for L-DOPA, which was incorporated by genetic-code reprogramming and thus might be subject to a negative selection pressure from lower translation efficiency. Given our interest in finding peptides that mimic the interactions of montbretin A with HPA and that the deep sequencing data showed two positions at which substitution with L-DOPA was tolerated, peptides with these substitutions were also synthesised and tested as HPA inhibitors (Table 3). Pleasingly, both positions showed improved

Table 3. Inhibition data for piHA-Dm containing L-DOPA.

Abbreviation	Structure/sequence	K_i [nM]
piHA-Dm-Y3d	cyclo(Ac-^{D}YP-*DOPA*-SC)WVRH-NH_2	0.48 ± 0.02
piHA-Dm-H9d	cyclo(Ac-^{D}YPYSC)WVR-*DOPA*-NH_2	3.7 ± 0.8
piHA-Dm-Y3d,V7A	cyclo(Ac-^{D}YP-*DOPA*-SC)WARH-NH_2	18 ± 3

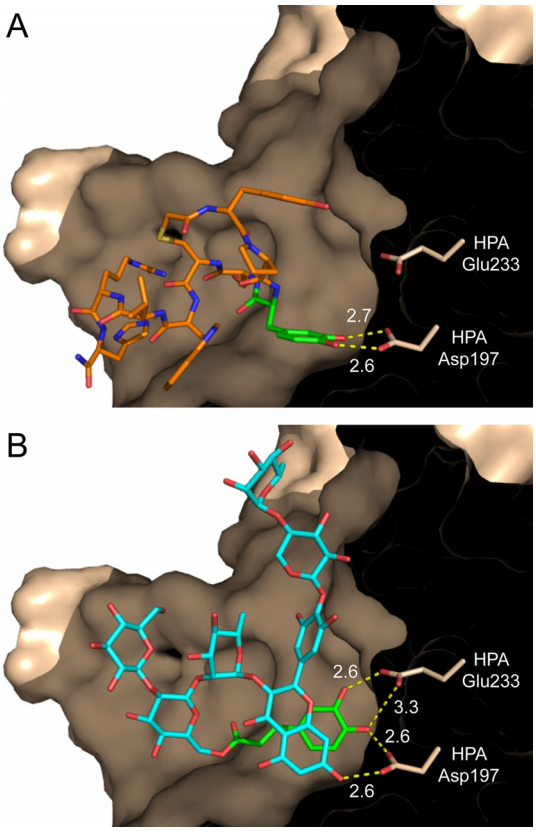

Figure 5. A) Model of bidentate L-DOPA interaction with HPA catalytic nucleophile Asp197 (orange, based on PDB ID: 5KEZ)[14] compared to B) the crystal structure of montbretin A interacting with the same residue as well as the catalytic acid/base Glu233 (cyan, PDB ID: 4W93).[11] Emphasised residues making multidentate interactions with catalytic residues are shown in green, with hydrogen bonds shown as dashed yellow lines and distances given in ångström. The surface and catalytic residues of HPA are shown in wheat tint, with heteroatoms coloured red for oxygen, blue for nitrogen, and yellow for cysteine.

K_i values by factors of approximately 2 for H9DOPA and 10 for Y3DOPA. The latter of these has the highest affinity for HPA of any peptide reported to date at 480 pM. Unexpectedly, combining the Y3DOPA and V7A mutations gave worse binding, despite each mutant separately giving higher affinity than piHA-Dm. These effects are thus clearly not additive. Nonetheless, this result is intriguing because whereas His9 is located at the outer edge of the active site and tolerates any aromatic amino acid, Tyr3 forms a specific hydrogen bond with the conserved catalytic nucleophile Asp197 of HPA[17] and tolerates no other natural amino acids.

Modelling of L-DOPA in the same location as Tyr3 by simple replacement of a hydrogen atom with a hydroxy group in our previously published crystal structure of piHA-Dm bound to HPA[14] suggests that a bivalent interaction would occur between these two amino acids. This is similar to that seen in montbretin A with Glu233 but in a slightly different location and lacking the contributions from the resorcinol moiety (Figure 5). Despite being slightly shifted, the catechol in L-DOPA indeed appears to be able to mimic the interactions of caffeic acid in montbretin A, as hoped. This result confirms the hypothesis that L-DOPA can form a strong bivalent interaction with catalytic carboxylate side chains in the active site of HPA and that the absence of peptides containing this residue in the enriched library is not from a lack of binding ability but rather from competing factors such as lower translation efficiency of the unnatural amino acid. This result also suggests that further work towards the goal of peptides mimicking montbretin A should focus on the resorcinol moiety, which would make a better mimic of myricetin, to realise the goal of a tuneable retaining glycosidase inhibition motif.

Conclusion

Together, the results showed that all consensus residues of a peptide inhibitor of human α-amylase (piHA-Dm) were important for its high affinity to human pancreatic α-amylase, and the most-important contribution to binding was from tyrosine 3, which was found to be situated adjacent to the catalytic residues of the enzyme. In addition to the many hydrogen bonds previously identified, aromatic interactions with Trp6 and His9 were also found to be important for high affinity. Evidence from CD experiments suggested that this peptide

adopts a 3_{10}-helical conformation in solution and is, thus, primed for binding to the human pancreatic α-amylase (HPA) active site. Substitution of the critical tyrosine 3 residue with L-DOPA, on the basis of careful analysis of deep sequencing data, afforded the highest affinity peptide inhibitor for this enzyme yet (K_i = 480 pM). Crucially, this increased affinity is likely the result of a bivalent hydrogen-bonding interaction with the catalytic nucleophile Asp197 of HPA. This result thus suggests it is possible to mimic one of the interactions seen in the natural product montbretin A by using a peptide scaffold, an important step towards tuning its potent inhibitory motif for other retaining glycosidases.

Experimental Section

Materials and equipment: Unless otherwise specified, reagents were purchased from Sigma–Aldrich or equivalent chemical retailers. Standard *N*-fluoren-9-ylmethoxycarbonyl (Fmoc) amino acids and reagents for peptide synthesis were purchased from GL Biochem (China), whereas Fmoc-L-DOPA(TBDMS)$_2$-OH (TBDMS = *tert*-butyldimethylsilyl) was synthesised by following literature procedures.[33] Peptide MALDI-TOF mass spectra were recorded by using a Kratos Analytical (UK) Axima-CFR. Enzyme kinetics were measured by using a BMG Labtech (Germany) POLARstar Omega plate reader, and UV spectra were measured with a Thermo Fisher Scientific (USA) Nanodrop 2000 for peptide solutions or UV1 for other compounds. CD spectra were recorded with an Olis (USA) RSM1000 by using a Hellma Analytics (Germany) 120QS quartz cuvette (path length: 2.0 mm).

Peptide synthesis and purification: Peptides were synthesised by using standard automated Fmoc solid-phase synthesis on RAPP polymere (Germany) tentagel S RAM resin with Symphony (Gyros protein technologies, USA) and Syro II (Biotage, Sweden) systems at scales of 100 and 25 μmol, respectively. Four equivalents of amino acid, 1-hydroxybenzotriazole (HOBt)/*N*-[(1*H*-benzotriazole-1-yl)(dimethylamino)methylene]-*N*-methylmethanaminium hexafluorophosphate *N*-oxide (HBTU), and *N*,*N*-diisopropylethylamine (DIPEA) were used in a single 40 min coupling step per round, with deprotection for 3 min with 40% piperidine and then for 10 min with 20% piperidine, all in DMF. Following completion of the synthesis, the peptides were capped on the N terminus with chloroacetyl-*N*-hydroxysuccinimide (NHS; 2×7.2 equiv) for 30 min in *N*-methylpyrrolidone (NMP), or for piHA-Dm-(lin) with acetic anhydride (6.25 equiv), DIPEA (1.6 equiv), and HOBt (0.19 equiv) in DMF. Side-chain-protecting TBDMS ethers in L-DOPA were removed by treatment with a solution of tetrabutylammonium fluoride (TBAF) in THF (600 μL, 180 mM, 4.3 equiv) for 5 min. Cleavage and global deprotection was by a 2 h reaction in a solution of 2.5% ethane-1,2-dithiol (EDT), 2.5% triisopropylsilane (TIPS), and 5% water in trifluoroacetic acid (TFA), and the cleavage solution was subsequently added dropwise to a 20-fold excess amount of ice-cold diethyl ether to precipitate the product. Cyclisation was performed by dissolving the dried crude peptide product to approximately 12.5 mM in DMSO and adding DIPEA until basic, then allowing the reaction to proceed at room temperature with monitoring by MS (MALDI-TOF) before quenching with a slight excess amount of TFA. The macrocyclic peptides were subsequently purified by preparative-scale HPLC by using a Phenomenex (USA) Gemini C_{18} column (250×21.1 mm, 10 μm) with a 10–70% gradient of acetonitrile in water (0.1% TFA as additive for both) over 40 min at 12.5 mL min^{-1} with UV monitoring. Product-containing fractions were identified by MS (MALDI-TOF) and were pooled if purity was assessed to be at least 95% by analytical HPLC with the same gradient at 1 mL min^{-1} with a Dr Maisch (Germany) Silicycle C_{18} column (150× 4.6 mm, 5 μm). Stocks of peptides containing L-DOPA were verified by MS (MALDI-TOF) not to be oxidised to any detectable degree over the time span of all experiments. For the L-DOPA monomer, the extinction coefficient was determined experimentally by using a 0.250 mM solution in sodium phosphate buffer pH 7.0 to be 2680 M^{-1} cm^{-1} (A = 0.671, l = 1 cm, n = 6 measurements). Peptide extinction coefficients were subsequently calculated from sequence by using a direct additive approach and the ExPASy protparam tool (https://web.expasy.org/protparam/protpar-ref.html).

Enzyme inhibition kinetics: Analysis of inhibition type such as by double reciprocal plots was not undertaken, as competitive inhibition by piHA-Dm was previously demonstrated and the X-ray crystal structure shows binding of piHA-Dm to the HPA active site.[14] IC_{50} values were first determined for all peptides by using a series of peptide concentrations spanning from 500 pM to 5 μM. Hydrolysis of 2-chloro-4-nitrophenyl-α-D-maltotrioside (4 mM) was monitored at λ = 405 nm in pH 7.0 sodium phosphate (50 mM) and sodium chloride (100 mM) at 30 °C. Reactions were monitored for 30 min and showed no apparent deviations from linearity over that time period. Peptides were allowed to preincubate with HPA for 5 min before adding substrate. Rate data were normalised to reactions without inhibitor, and these data were then fit by using GraphPad (USA) Prism 7 ("[inhibitor] vs. response (three parameters)" equation, with the lower limit additionally constrained to 0). In cases for which tight binding inhibition was observed, K_i values were subsequently determined. Given that the K_i values for these peptides approach or are lower than the enzyme concentrations required for an observable signal, and thus the assumptions of Michaelis–Menten kinetics do not hold true, the Morrison method for tight binding inhibitors[34] was used with the enzyme and peptide concentrations as indicated in each plot (Supporting Information). Fitting of these data was performed by using the same software ("Morrison K_i" equation, with K_M constrained to 3.6 mM).

Circular dichroism: Freeze-dried peptides were dissolved to approximately 50 μM in the HPA kinetics buffer detailed above (additionally containing 0.5 or 2.0 M guanidinium hydrochloride as required), allowed to equilibrate at 4 °C overnight, and then centrifuged to remove the debris. Spectra were collected at 20 °C under a nitrogen atmosphere in steps of 1 nm from λ = 190 to 250 nm with an integration time of 10 s, and then the concentration of the peptide solution was determined to convert into per-residue molar ellipticity. A background spectrum of buffer alone was subtracted in all cases, and an additional five-point moving average smoothing effect was applied to the raw data.

Deep sequencing analysis: Crude sequence data was extracted and converted into a list of peptide sequences and was then analysed by python script to extract variants at each sequence position (for script, see the Supporting Information). Raw sequence counts at each position were subsequently converted into percentage abundance.

Acknowledgements

We would like to thank Prof. Stephen G. Withers (University of British Columbia) for kindly providing deglycosylated recombinant human pancreatic α-amylase and 2-chloro-4-nitrophenyl-α-D-maltotrioside, Dr. John Kruijtzer (Utrecht University) for assis-

tance with peptide synthesis, and Utrecht University for financial support.

Conflict of Interest

The authors declare no conflict of interest.

Keywords: carbohydrates · enzymes · inhibitors · natural products · peptides

[1] A. Varki, *Glycobiology* **2017**, *27*, 3 – 49.
[2] V. Lombard, H. Golaconda Ramulu, E. Drula, P. M. Coutinho, B. Henrissat, *Nucleic Acids Res.* **2014**, *42*, D490 – D495.
[3] J. Rini, J. Esko, A. Varki, *Glycosyltransferases and Glycan-Processing Enzymes*, Cold Spring Harbor Laboratory Press, New York, **2009**.
[4] T. M. Gloster, D. J. Vocadlo, *Nat. Chem. Biol.* **2012**, *8*, 683 – 694.
[5] T. M. Gloster, G. J. Davies, *Org. Biomol. Chem.* **2010**, *8*, 305 – 320.
[6] T. Passioura, H. Suga, *Chem. Commun.* **2017**, *53*, 1931 – 1940.
[7] J. Morimoto, Y. Hayashi, H. Suga, *Angew. Chem. Int. Ed.* **2012**, *51*, 3423 – 3427; *Angew. Chem.* **2012**, *124*, 3479 – 3483.
[8] Y. Matsunaga, N. K. Bashiruddin, Y. Kitago, J. Takagi, H. Suga, *Cell Chem. Biol.* **2016**, *23*, 1341 – 1350.
[9] A. Kawamura, M. Münzel, T. Kojima, C. Yapp, B. Bhushan, Y. Goto, A. Tumber, T. Katoh, O. N. F. King, T. Passioura, L. J. Walport, S. B. Hatch, S. Madden, S. Müller, P. E. Brennan, R. Chowdhury, R. J. Hopkinson, H. Suga, C. J. Schofield, *Nat. Commun.* **2017**, *8*, 14773.
[10] Y. Hayashi, J. Morimoto, H. Suga, *ACS Chem. Biol.* **2012**, *7*, 607 – 613.
[11] L. K. Williams, X. Zhang, S. Caner, C. Tysoe, N. T. Nguyen, J. Wicki, D. E. Williams, J. Coleman, J. H. McNeill, V. Yuen, R. J. Andersen, S. G. Withers, G. D. Brayer, *Nat. Chem. Biol.* **2015**, *11*, 691 – 696.
[12] N. N. Mhlongo, A. A. Skelton, G. Kruger, M. E. S. Soliman, I. H. Williams, *Proteins Struct. Funct. Bioinf.* **2014**, *82*, 1747 – 1755.
[13] H. G. Preuss, *J. Am. Coll. Nutr.* **2016**, *28*, 266 – 276.
[14] S. A. K. Jongkees, S. Caner, C. Tysoe, G. D. Brayer, S. G. Withers, H. Suga, *Cell Chem. Biol.* **2017**, *24*, 381 – 390.
[15] C. A. Tarling, K. Woods, R. Zhang, H. C. Brastianos, G. D. Brayer, R. J. Andersen, S. G. Withers, *ChemBioChem* **2008**, *9*, 433 – 438.
[16] A. J. Scheen, *Drugs* **2003**, *63*, 933 – 951.
[17] G. D. Brayer, Y. Luo, S. G. Withers, *Protein Sci.* **1995**, *4*, 1730 – 1742.
[18] G. D. Brayer, G. Sidhu, R. Maurus, E. H. Rydberg, C. Braun, Y. Wang, N. T. Nguyen, C. M. Overall, S. G. Withers, *Biochemistry* **2000**, *39*, 4778 – 4791.
[19] E. H. Rydberg, C. Li, R. Maurus, C. M. Overall, G. D. Brayer, S. G. Withers, *Biochemistry* **2002**, *41*, 4492 – 4502.
[20] M. Qian, R. Haser, G. Buisson, E. Duée, F. Payan, *Biochemistry* **1994**, *33*, 6284 – 6294.
[21] G. Wiegand, O. Epp, R. Huber, *J. Mol. Biol.* **1995**, *247*, 99 – 110.
[22] C. Tysoe, L. K. Williams, R. Keyzers, N. T. Nguyen, C. Tarling, J. Wicki, E. D. Goddard-Borger, A. H. Aguda, S. Perry, L. J. Foster, R. J. Andersen, G. D. Brayer, S. G. Withers, *ACS Cent. Sci.* **2016**, *2*, 154 – 161.
[23] S. Strobl, K. Maskos, G. Wiegand, R. Huber, F. X. Gomis-Rüth, R. Glockshuber, *Structure* **1998**, *6*, 911 – 921.
[24] B. Svensson, K. Fukuda, P. K. Nielsen, B. C. Bønsager, *Biochim. Biophys. Acta Proteins Proteomics* **2004**, *1696*, 145 – 156.
[25] S. A. K. Jongkees, S. Umemoto, H. Suga, *Chem. Sci.* **2017**, *8*, 1474 – 1481.
[26] K. Iwasaki, Y. Goto, T. Katoh, H. Suga, *Org. Biomol. Chem.* **2012**, *10*, 5783 – 5786.
[27] S. A. K. Jongkees, C. J. Hipolito, J. M. Rogers, H. Suga, *New J. Chem.* **2015**, *39*, 3197 – 3207.
[28] N. H. Andersen, Z. Liu, K. S. Prickett, *FEBS Lett.* **1996**, *399*, 47 – 52.
[29] C. Toniolo, A. Polese, F. Formaggio, M. Crisma, J. Kamphuis, *J. Am. Chem. Soc.* **1996**, *118*, 2744 – 2745.
[30] E. Schievano, A. Bisello, M. Chorev, A. Bisol, S. Mammi, E. Peggion, *J. Am. Chem. Soc.* **2001**, *123*, 2743 – 2751.
[31] S. M. Howell, S. V. Fiacco, T. T. Takahashi, F. Jalali-Yazdi, S. W. Millward, B. Hu, P. Wang, R. W. Roberts, *Sci. Rep.* **2014**, *4*, 6008.
[32] F. Jalali-Yazdi, L. Huong Lai, T. T. Takahashi, R. W. Roberts, *Angew. Chem. Int. Ed.* **2016**, *55*, 4007 – 4010; *Angew. Chem.* **2016**, *128*, 4075 – 4078.
[33] M. J. Sever, J. J. Wilker, *Tetrahedron* **2001**, *57*, 6139 – 6146.
[34] J. F. Morrison, *Biochim. Biophys. Acta Enzymol.* **1969**, *185*, 269 – 286.

Manuscript received: August 26, 2017
Accepted manuscript online: October 6, 2017
Version of record online: November 7, 2017